Topology optimization with displacement constraints: a comparative analysis of acetabular cage designs and bone graft's strain energy density

Martin Olivér Dóczi*, Péter Tamás Zwierczyk

Department of Machine and Product Design, Faculty of Mechanical Engineering, Budapest University of Technology and Economics, Hungary

DOI: 10.17489/biohun/2023/1/582

Abstract

Large acetabular defects can be treated effectively through the use of acetabular cages combined with bone grafts, with the formation of living bone facilitated by mechanical stimulus. The mechanical stimulus on the graft is highly dependent on the design of the acetabular cage. Topology optimization offers a means to create conceptual designs of acetabular cages, which can then be assessed for their impact on strain energy density (SED) distribution within the graft. This study aims to compare various acetabular cage designs generated through multiple optimization constraints, with a focus on analyzing the SED distribution in the graft.

A virtual bone defect was modeled, and a graft was virtually implanted within it, followed by the creation of a design space for the acetabular cage. Different acetabular cup designs were then generated using volume minimization as the objective function, along with varying displacement constraints, namely the global displacement of the cage center or its relative displacement to the pelvis constrained. Linear static simulations were performed on the hemipelvis model, and the results were filtered using different relative densities to evaluate SED distribution in the graft.

The results revealed that the acetabular cage designs produced qualitatively similar strain energy density distributions. Both types of optimization are worth using because together they were able to reduce the element-wise average SED relative errors to below 14%. The model using relative displacement constraints can produce more diverse acetabular cage variants than the model with global displacement constraints.

Keywords: acetabular cage, topology optimization, finite element method, graft transformation

***Corresponding author contact data:** Department of Machine and Product Design, Faculty of Mechanical Engineering, Budapest University of Technology and Economics. Műegyetem rkp. 3., H-1111 Budapest, Hungary. **E-mail:** doczi.martin@gt3.bme.hu **Tel.:** +36 1 463-1372

Citation: *Dóczi MO, Zwierczyk PT. Topology optimization with displacement constraints: a comparative analysis of acetabular cage designs and bone graft's strain energy density. Biomech Hung. 2023;16(1):7-16.*

Received: 28/04/2023 **Accepted:** 18/06/2023

1. Introduction

Acetabular defects, commonly caused by trauma, infection, or other medical conditions, can result in significant disability and reduced quality of life for affected individuals.[1,2] One potential treatment option for addressing these defects is the use of acetabular cages. These cages often involve the incorporation of bone grafts, which can help restore function and stability to the hip joint. The success of bone grafting procedures depends on multiple factors, such as the quality and quantity of bone used and the mechanical stimulus on the graft during the healing process.

In the existing literature[1,3-5] numerous treatment methods have been proposed, with bone grafts being employed to manage bone deficiencies.

Finite element (FE) methods have been utilized to examine acetabular cages with typical models in the literature.[6-10] These share the commonality that the boundary conditions are imposed as fixed constraints at the pubic joint and the sacroiliac joint and active force application at the center of the acetabular cage. These FE methods allow for efficient examination of the stress state of the acetabular cage.

Topological optimization techniques have also been employed in the design of acetabular cages. Notably, the work of Iqbal et. al.[11] has been significant in this area, with a focus on replacing bone deficiencies resulting from cancerous conditions. In these topologically optimized designs, the aim is to maximize stiffness and bridge extensive defects with acetabular cages.

Although this stiffness-maximization approach can produce useful cage concepts, the literature generally lacks studies that advocate for more optimal graft transformation. Challenges such as uncertainties and high computational demands must be addressed. Notable is the study of Wu et al. about the mandible.[12] In the studies[12-14] of bone- bone graft transformations, models typically associate the extent of transformation with the change in strain energy density (SED). In a study[15] focusing on the acetabular side, three load vectors were identified, the average of which was found to represent the equivalent effect of the entire life activity spectrum.

The objective of this research is to explore the potential of using a reduced model with varying constraints to create conceptual acetabular cup designs and to determine how these designs can be produced using alternative models. Furthermore, this study aims to evaluate the performance of these acetabular cage concepts within a hemipelvis model and assess the similarity of SED distributions generated within the graft.

2. Methods

2.1. Overall procedure

The overall procedure can be seen in *Figure 1*. The finite element method was used for solving the task. Three acetabular cage variants were generated on a reduced model, using topology optimization with different displacement constraints for the center of the acetabular cage. A relative density of 0.8 was used to query the results of the topology optimization. The goal was to create multiple variants quickly, each with a unique visual appearance. These resultant conceptual designs were then evaluated in the hemipelvis model using second-order elements. These are the reference models. The evaluated results were the displacements of the center of the acetabular cage in the x, y, and z directions, as well as the relative displacements compared to the three points of the pelvis. Subsequently, two types of

models were created: one that constrained the global displacements of the acetabular cage within +/- 10% of the reference values (6 constraints) for the three unit loads and another, that constrained the relative displacements (9 constraints) with the same range. For the evaluation of SED distributions, the following vector triplet in the reference[15] was chosen, and the average SED response for this vector triplet was plotted.

Linear static simulations were performed on the hemipelvis model to evaluate the distribution of strain energy density in the graft for each acetabular design. The simulations and the optimization calculations were conducted using OptiStruct 2020.1.

The details of this process are discussed in the following subsections.

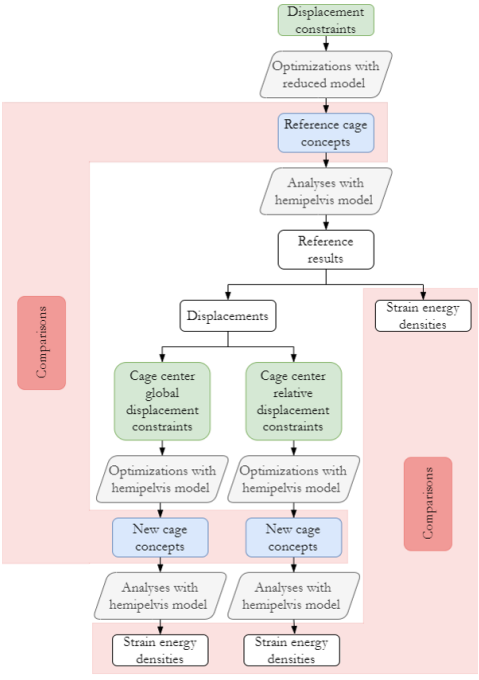

Figure 1. The overall procedure

2.2. CAD design

A virtual bone defect was created by segmenting a healthy pelvis model with Slicer 3D and removing a portion of the acetabulum, resulting in a bone defect that was representative of a typical acetabular defect using Autodesk Meshmixer. A graft was then virtually implanted into the defect, and the design space for the acetabular cage was modeled in Solidworks 2020. Care was taken to ensure that the possible placement of the acetabular cage did not significantly exceed the dimensions of a healthy pelvis. The design space was configured such that it does not connect to the region behind the acetabular cage. This enables much broader optimization result possibilities and facilitates the creation of sheet metal-like models. *Figure 2* demonstrates the CAD model.

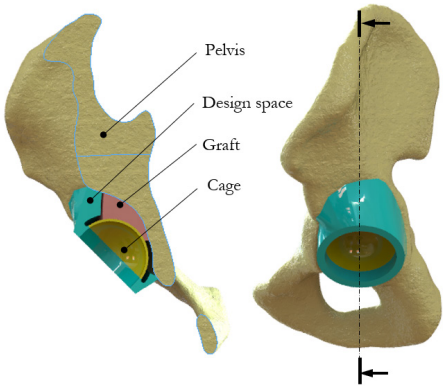

Figure 2. The CAD model of the fixation

2.3. Finite element modeling

The preprocessing was carried out in HyperMesh. First, the hemipelvis FE model is introduced, and then the differences between the reduced model and the hemipelvis model are discussed.

The pelvic bone was separated into cortical and cancellous bone compartments. The cor-

tical bone compartment was modeled using 1 mm thick shell elements.[6] Solid elements were used everywhere else and the mesh shared common nodes to each part (bonded connection). For the topology optimization models, first-order elements were used for faster execution, while second-order elements were used for the analyses to ensure accuracy. Homogeneous, linear elastic, and isotropic material models were used for all materials. The material of the acetabular cage was stainless steel. The material properties used during the simulations can be found in *Table 1*, the relevant details of the FE mesh (number of nodes and elements) are in *Table 2*.

Table 1. The material properties

Name	Young's modulus [MPa]	Poisson's ratio [-]
Steel (acetabular cage)	192 000	0.3
Corticalis bone[6,16]	17 000	0.3
Spongiosus bone[16]	200	0.3
Graft[16]	115.2	0.3

Table 2. The details of the FE mesh

Name	Value
Number of elements in the reduced model	990 400
Number of elements in the hemipelvis model	1 026 750
Number of nodes in the design space	136 641
Number of elements in the design space	813 058
Number of nodes in the graft (for analysis)	66 121
Number of elements in the graft (for analysis)	48 295
Max. aspect ratio in the graft	4.66

In the case of the hemipelvis model, constraints were applied at the pubic symphysis and the sacroiliac joint.[6,7] In the case of the reduced model, the model size was reduced according to *Figure 3*, and fixed constraints were applied to the surfaces from the omitted parts. The loads were applied at the center of the acetabular cage and were transferred to the rest of the cage through rigid elements. The coordinate system was the same as what Bergmann et al. used in their work.[17]

Information on the loads can be found in *Table 3*. Unit loads played a more significant role in the topology optimization, while the other three loads were used for determining the SED distributions.[15]

2.4. Topology optimization model

Volume minimization involves minimizing the total volume of material used in the design subject to certain constraints. This approach aims to remove all non-essential material from the design, resulting in a lighter and more efficient structure. During preliminary attempts, models created with stiffness maximization, volume fraction constraint, and displacement

Table 3. The loads in the FE model

#	Name	Force component x [N]	Force component y [N]	Force component z [N]
1	Unit load x direction	1 000	0	0
2	Unit load y direction	0	1 000	0
3	Unit load z direction	0	0	1 000
4	Load for graft transformation I.[15]	363.7455	0	1 444.023
5	Load for graft transformation II.[15]	68.79838	0	1 444.023
6	Load for graft transformation III.[15]	128.3141	-356.8297	298.8481

constraints did not achieve the desired results, as they were only able to meet the requirements with significant discontinuities after lengthy iterations. In contrast, volume minimization with displacement constraint proved to be convergent.

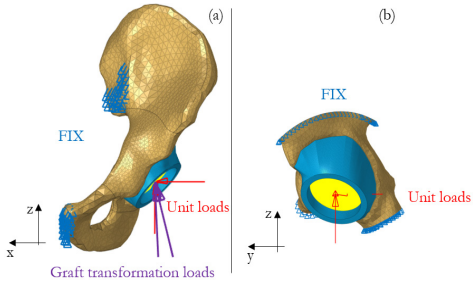

Figure 3. The FE models: Hemipelvis (a), reduced model (b)

The rotations were not constrained. They were small anyway, and with many extra constraints, it was feared that the simulation would not converge. To create reference models, the reduced model was used for its speed. Here, the displacements were recorded for the three acetabular cage variants. The initial topology optimization was performed using the reduced model as well. In this stage, the three different cage variants were generated, and their displacements were analyzed in the hemipelvis model. Volume minimization with Solid Isotropic Material Penalization (SIMP) method[18] with displacement constraint was used to create these cage variants.

The preliminary displacement constraints prescribed on the reduced model can be seen in *Table 4*.

The aim was to quickly create different acetabular cage variants within the design space. By analyzing these variants, the displacements were obtained that were used to constrain the optimization model built using the hemipelvis model. The figure showing the full model is *Figure 4* with the relative distances of the hemipelvis.

These displacement constraints can be divided into two groups.

Global displacements constrain the center of the acetabular cage. In this case, the displace-

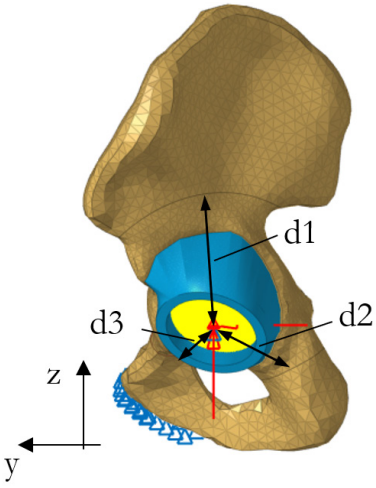

Figure 4. The hemipelvis optimization model marked with the relative distances

Table 4. Preliminary displacement constraint for the reduced model

Name	Bound	Displacement x for unit load x	Displacement y for unit load y	Displacement z for unit load z
Red. model I.	Lower bound	0 mm	0 mm	0.02 mm
	Upper bound	0.03 mm	0.03 mm	0.03 mm
Red. model II.	Lower bound	0 mm	0 mm	0.02 mm
	Upper bound	0.04 mm	0.04 mm	0.03 mm
Red. model III.	Lower bound	0 mm	0 mm	0.01 mm
	Upper bound	0.04 mm	0.04 mm	0.02 mm

ment responses to the unit loads can be written in a symmetric matrix, and thus six constraints were prescribed, namely, that the obtained displacements must be within +/- 10% of their lower and upper limits. Regarding the constraint of relative displacements, points were selected slightly farther away from the acetabular cage but still close to the center of the cutting surface of the reduced models, and the change in their distances was examined. The optimization constraints were set so that the deviation of these distance changes could only be within +/- 10%. These displacement constraints can be seen in *Table 5*. The unit loads are shown in the columns. The lower and upper limits are separated by a slash. The letter before the limits represents the direction for global displacement constraints, while for relative displacement constraints, the letter specified in *Figure 4* is used to identify the measured distance.

The relevant constant parameters for all optimizations are presented in *Table 6*.

3. Results

The post-processing was carried out using HyperView. *Figure 5* presents the resulting acetabular cage variants with different relative densities.

Table 6. Parameters for the optimizations

Name	Value
Minimum dimension	7 mm
Initial material fraction	0.6
Minimum element material density	0.001
Discreteness parameter	5
Relative convergence criterion	3%

Figure 6 displays the SED distributions of the different models.

Table 7 shows the average- and median values of the deviations.

Table 5. Displacement constraints for the hemipelvis model

Name	For unit load x [mm]	For unit load y [mm]	For unit load z [mm]
Hemipelvis global model I.	dx: 0.0927/0.113	-	-
	dy: -0.0669/-0.0547	dy: 0.3569/0.4362	-
	dz: -0.0109/-0.0099	dz: 0.0807/0.0986	dz: 0.0887/0.1084
Hemipelvis global model II.	dx: 0.1012/ 0.1237	-	-
	dy: -0.0683/ -0.0559	dy: 0.3826/ 0.4677	-
	dz: -0.0114/ -0.0093	dz: 0.0827/ 0.1011	dz: 0.0886/ 0.1083
Hemipelvis global model III.	dx: 0.0968/ 0.1184	-	-
	dy: -0.0588/ -0.0481	dy: 0.3531/ 0.4316	-
	dz: -0.0126/ -0.0103	dz: 0.0764/ 0.0934	dz: 0.0808/ 0.0987
Hemipelvis rel. disp. model I.	d1: -0.0030/ -0.00241	d1: -0.0270/ -0.0221	d1: -0.0401/ -0.0328
	d2: -0.0042/ -0.0034	d2: 0.0057/ 0.0070	d2: 0.0024/ 0.0029
	d3: -0.0333/ -0.0273	d3: -0.0358/ -0.0293	d3: 0.0015/ 0.0018
Hemipelvis rel. disp. model II.	d1: -0.0020/ -0.0017	d1: -0.0326/ -0.0267	d1: -0.0389/ -0.0318
	d2: -0.00684/-0.0056	d2: 0.0097/ 0.0118	d2: 0.0023/ 0.0029
	d3: -0.0428/ -0.0351	d3: -0.0462/ -0.0378	d3: 4.61e-05/ 5.63e-05
Hemipelvis rel. disp. model III.	d1: -0.0039/ -0.0032	d1: -0.0134/ -0.0110	d1: -0.0256/ -0.0210
	d2: -0.0103/ -0.0084	d2: 0.0100/ 0.0122	d2: 0.0020/ 0.0025
	d3: -0.0410/ -0.0335	d3: -0.0445/ -0.0364	d3: 0.0011/ 0.0013

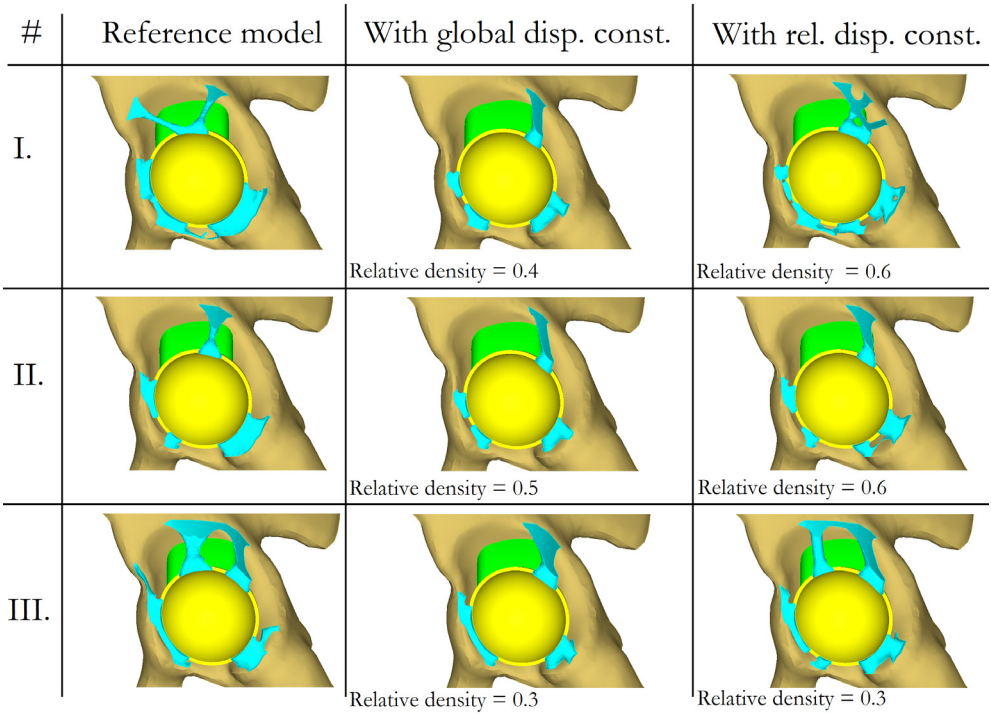

Figure 5. Resultant acetabular cage variants compared to the reference model

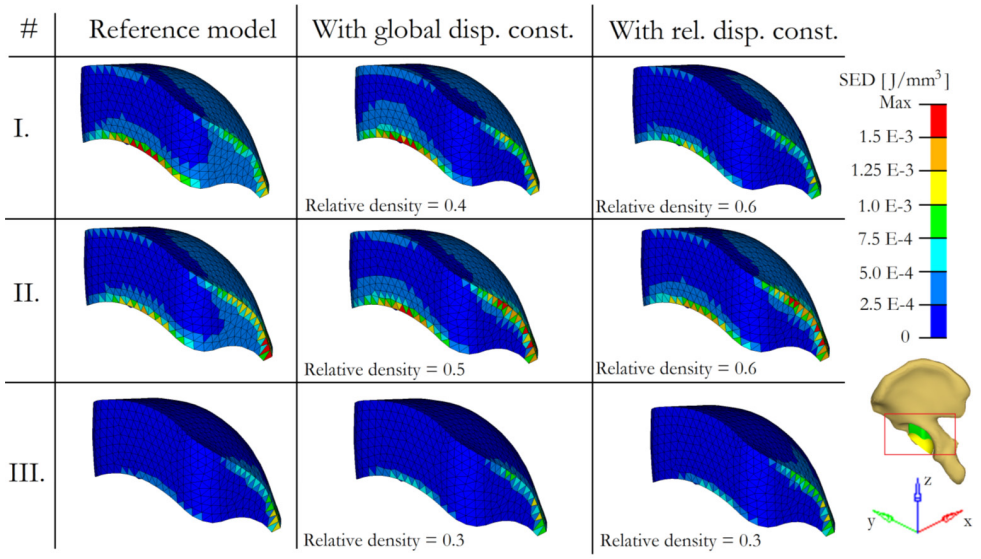

Figure 6. SED distributions of the graft in the models

4. Discussion

It can be observed that the acetabular cage variants created by the models constrained by global displacements were fairly uniform and resembled the second reference model. However, the models created with relative displacement constraints were more diverse and showed a greater similarity to the reference models, with the exception of the result related to the first reference model. For the first model, both the reference model and the one created with relative displacement constraints had in common that more material was added to the lower part of the acetabular cage in an attempt to limit horizontal displacements. The choice of relative density, i.e., which parts to consider from the results of the topology optimization, also plays a significant role in the outcomes. By testing multiple relative density values and evaluating the average deviation, the values were chosen with the aim of minimizing the average deviation. The simulations were carried out with a relative density accuracy of one decimal place. In the case of the global model III., it was not particularly observed that it followed the reference model's SED distribution, regardless of the relative density. In each case, a similar SED distribution was developed in the grafts. The first model, where the global displacement-based constraint was used achieved a smaller average error, while in the third model, the relative displacement-based constraint performed better. In the third case, the improvement is significant because the relative displacement-based optimization also captured the topology of the cage.

It should be noted that the current acetabular cage variants are still conceptual in nature, and the actual stiffness connections will modify the SED distribution. This is a significant limitation of the current study besides the completely linear model. Future plans include generating desirable SED distributions even more rapidly and with even simpler models, followed by attempting to approximate these distributions using conceptual acetabular cage variants constrained by relative displacements. Further investigations using other models would be beneficial, with different design space and defect geometry.

Table 7. The average- and the median values of SED relative deviations

Model name	Average values of deviations	Median values of deviations
Hemipelvis global model I.	14%	9%
Hemipelvis global model II.	19%	11%
Hemipelvis global model III.	32%	16%
Hemipelvis rel. disp. model I.	25%	9%
Hemipelvis rel. disp. model II.	12%	7%
Hemipelvis rel. disp. model III.	10%	8%

5. Conclusions

The models that were constrained by relative displacements resulted in acetabular cage variants that were conceptually similar to the reference models. In the case of models that were constrained by global displacements, very similar and uniform solutions were obtained, due to the close values of the displacement constraints. The average deviations between the SED distributions of the constrained models and the reference models were found to be between 12% to 14%, which is considered acceptable given the +/- 10% displacement constraints. The model using relative displacement constraints can produce more diverse acetabular cage variants than the model with global displacement constraints. After checking their strength, a much more accurate insight can be obtained of what kind of cage topology would be ideal.

Author contributions: M.O.D. conducted the literature review, developed the FE and the topology optimization model, ran the simulations, and wrote the manuscript. P.T.Z. gave feedback on the FE model results and gave feedback on the manuscript.

Funding: Project no. TKP-9-8/PALY-2021 has been implemented with the support provided by the Ministry of Culture and Innovation of Hungary from the National Research, Development and Innovation Fund, financed under the TKP2021-EGA funding scheme.

Conflict of interest: None

Abbreviations: CAD – computer-aided design, FE – finite element, SED – strain energy density

References

1. *Ahmad A, Schwarzkopf R.* Clinical evaluation and surgical options in acetabular reconstruction: A literature review. J Orthop. 2015;12(2):S238-S243. DOI
2. *Paprosky W, Perona P, Lawrence J.* Acetabular defect classification and surgical reconstruction in revision arthroplasty: A 6-year follow-up evaluation. J Arthroplasty. 1994;9(1):33-44. DOI
3. *Sződy R, Kotormán I, Manó S, et al.* Csípőprotézis revízióikor alkalmazott „custom made" vápakosár tervezése és készítése, három esetben alkalmazott eljárás. 7th Hungarian Conference of Biomechanics; 2017 Oct 6-7; Szeged, Hungary. (in Hungarian)
4. *Bejek Z, Lakatos J, Skaliczki G, Szendrői M.* Vápa-rekonstrukciós lehetőség kiterjedt os ilii defektus esetén revíziós műtétekben. Magy Traumatol Ortop Kezseb Plasztikai Seb. 2014;57(1):27-32. (in Hungarian)
5. *Schreurs BW, Slooff TJ, Gardeniers JW, Buma P.* Acetabular Reconstruction With Bone Impaction Grafting and a Cemented Cup: 20 Years' Experience. Clin Orthop Rel Res. 2001;339:202-215. DOI
6. *Plessers K, Mau H.* Stress analysis of a Burch-Schneider cage in an acetabular bone defect: A case study. Reconstructive Review. 2016;6(1):37-42. DOI
7. *Dóczi M, Sződy R, Zwierczyk PT.* Failure analysis of a custom-made acetabular cage with finite element method. In: *Steglich M, Mueller C, Neumann G, Walther M, editors.* ECMS 2020. Proceedings of the 34th International ECMS Conference on Modelling and Simulation; 2020 Jun 9-12; Wildau, Germany: European Council for Modelling and Simulation. p. 250-255. DOI
8. *Vogel D, Klimek M, Saemann M, Bader R.* Influence of the acetabular cup material on the shell deformation and strain distribution in the adjacent bone - a finite element analysis. Materials. 2020;13:1372. DOI
9. *Totoribe K, Chosa E, Yamako G, et al.* Acetabular reinforcement ring with additional hook improves stability in three-dimensional finite element analyses of dysplastic hip arthroplasty. J Orthop Surg Res. 2018;13:313. DOI
10. *Fu J, Ni M, Chen J, et al.* Reconstruction of severe acetabular bone defect with 3D printed Ti6Al4V augment: A finite element study. BioMed Res Int. 2018;2018:6367203. DOI
11. *Iqbal T, Wang L, Li D, et al.* A general multi-objective topology optimization methodology developed for customized design of pelvic prostheses. Med Eng Phys. 2019;69:8-16. DOI
12. *Wu C, Zheng K, Fang J, Steven GP, Li Q.* Time-dependent topology optimization of bone plates considering bone remodeling. Comput Methods Appl Mech Eng. 2020;359:112701. DOI
13. *Huiskes R, Weinans H, Grootenboer HJ, et al.* Adaptive bone-remodeling theory applied to prosthetic-design analysis. J Biomech. 1987;20(11-12):1135-1150. DOI
14. *Mirulla AI, Pinelli S, Zaffagnini S, et al.* Numerical simulations on periprosthetic bone remodeling: a systematic review. Comput Methods Programs Biomed. 2021;204:106072. DOI

15. *Dóczi MO, Sződy R, Zwierczyk PT.* Equivalent loads from the life-cycle of acetabular cages in relation to bone-graft transformation. Comput Methods Programs Biomed. 2023;236:107564. DOI
16. *Anderson AE, Peters CL, Tuttle BD, Weiss JA.* Subject-specific finite element model of the pelvis: Development, validation and sensitivity studies. J Biomech Eng. 2005;27(3):364-37. DOI
17. *Bergmann G, Deuretzbacher G, Heller M, et al. Hip contact forces and gait patterns from routine activities. J Biomech. 2001;34(7):859-891.* DOI
18. *Bendsøe MP.* Optimal shape design as a material distribution problem. Struct Optim. 1989;1:193-202. DOI